Polylactic Acid Bionanocomposites Filled with Nanocrystalline Cellulose from TEMPO-Oxidized Oil Palm Lignocellulosic Biomass

Eti Indarti,[a,b] Rohaizu Roslan,[a] Marwan,[c] and Wan Rosli Wan Daud [a,*]

Bionanocomposites from polylactic acid (PLA) filled with unmodified nanocrystalline cellulose from TEMPO-oxidized oil palm empty fruit bunch (OPEFB-NCC) at various loading levels were fabricated using the solvent casting technique. Scanning electron microscopy (SEM), transmission electron microscopy (TEM), attenuated total reflectance Fourier transform infrared spectroscopy (ATF-FTIR), differential scanning calorimetry (DSC), and mechanical analyses were used to characterize the bionanocomposite films. FTIR suggested that the incorporation of the OPEFB-NCC was based on physical interaction. The melting temperature did not change markedly except at higher OPEFB-NCC additions, while the crystallization temperature shifted to lower temperatures and crystallinity increased with increasing OPEFB-NCC content.The SEM of cryo-fractured films indicated a rather weak compatibility between the OPEFB-NCC and PLA, resulting in the decrease of both the modulus and the tensile strength of the bionanocomposite.

Keywords: OPEFB; Nanocrystalline cellulose; Polylactic acid; TEMPO-oxidation; Bionanocomposites

Contact information: a: Bioresource, Paper and Coating Division, School of Industrial Technology, Universiti Sains Malaysia, 11800 USM, Penang, Malaysia; b: Agricultural Product Technology Dept., Faculty of Agriculture, Syiah Kuala University, Banda Aceh 23111, Indonesia; c: Chemical Engineering Dept., Faculty of Engineering, Syiah Kuala University, Banda Aceh 23111, Indonesia;
**Corresponding author: wanrosli@usm.my*

INTRODUCTION

In recent years, research in biopolymer composites has gained great momentum due to increasing environmental concerns about the use of petroleum-based materials. Polylactic acid (PLA) has been touted as the most promising polymer because of its renewability, biodegradability, compatibility, and excellent transparency (Frone *et al*. 2013). However, PLA has its shortcomings, such as low thermal resistance, brittleness, poor resistance to gas and water vapor permeability, and low crystallization speed (Fortunati *et al*. 2012a). Moreover, compared with other commercial polymers, its price is relatively high (Avérous and Halley 2009). To reduce these problems, PLA has been blended with various biodegradable polymers such as starch (Shirai *et al*. 2013) and cellulose (Raquez *et al*. 2013). Due to the unique properties of cellulose, such as its non-toxicity, swelling ability, and stability under variations in temperature and pH, this natural material has been extensively studied for enhancing the PLA properties (Cheng *et al*. 2011). Among the various types of cellulosic materials such as pulp, microcrystalline cellulose (MCC), and nanocrystalline cellulose (NCC), the latter seems to generate considerable interest due to its ability to improve mechanical and barrier properties of PLA biocomposites; these effects are related to the high specific area and Young's modulus (145

to 150 GPa) of NCC (Miao and Hamad 2013). An inherent problem with NCC that limits its use to only aqueous or polar processes is its dispersibility and incompatibility with most polymeric matrices, which necessitates chemical modifications such as adsorbed surfactant (Heux *et al*. 2000), graft polymerization (Lin *et al*. 2009), and silane treatment (Gousséet *al*. 2002). All of these, however, involve chemical treatments, and it would be of considerable importance if unmodified NCC could be used for this purpose. Developing an unmodified NCC product is the object of the present work.

NCC is composed of rod-like particles that are 100 to 500 nm long and less than 10 nm in width (Habibi *et al*. 2010). It can be isolated from a variety of cellulose sources, both woody (Beck-Candanedo *et al.* 2005) and non-woody (Mandal and Chakrabarty 2011), with the former being the primary source. As one of the world's biggest producers of palm oil, Malaysia has an abundant supply of oil palm biomass comprising empty fruit bunches (OPEFB), fibers, shells, wet shells, palm kernels, fronds, and trunks. These residues represent an abundant, inexpensive, and readily available source of cellulose from a renewable biomass which has the potentials to be exploited into value-added products. In this study, NCC, which was isolated from OPEFB via the sono-assisted TEMPO-mediated oxidation was used as fillers in bionanocomposites with polylactic acid as the polymer matrix. To the best of our knowledge, this is the first report that deals with such investigation.

NCC is usually isolated from the crystalline regions of cellulose fibers *via* strong acid hydrolysis, primarily using sulfuric acid at elevated temperatures (Bondeson *et al*. 2006).This method produces surface negative charges by way of the sulphate groups that are induced during the reactions, which improve the dispersibility because aggregation is prevented by the electrostatic repulsion between the particles.Apart from participating in a corrosive system, another disadvantage of acid hydrolysis is its relatively low yield (30%). NCC has also been prepared from cellulose using 2,2,6,6-tetramethylpiperidine-1-oxy (TEMPO)-mediated oxidation followed by mechanical disintegration. The TEMPO radical helps to introduce additional carboxylic groups onto the fibers, thus allowing them to form dispersions of individualized fibers in water (Johnson *et al*. 2009). In additionto the induction of a negatively charged surface, the TEMPO-oxidation method is also advantageous due to its production of oxidized yields of up to 90%. A general reaction scheme of the oxidation of C6 hydroxyl to the carboxyl group by the TEMPO treatment is shown in Fig. 1.

This study investigated the use of unmodified NCC that was isolated from OPEFB (OPEFB-NCC) using the TEMPO-mediated process (Rohaizu and Wanrosli 2017) as fillers in PLA bionanocomposites. These materials were characterized using scanning electron microscopy (SEM), transmission electron microscopy (TEM), Fourier transform infrared spectroscopy (FTIR), differential scanning calorimetry (DSC), and mechanical analyses.

EXPERIMENTAL

Material

The raw material used for the preparation of OPEFB-NCC was OPEFB fibrous strands, sourced from SABUTEK (M) Sdn. Bhd. Teluk Intan, Perak, Malaysia. A 98% solution of 4-acetamido-TEMPO (2,2,6,6-tetramethylpiperidin-1-oxyl) was obtained from Sigma-

Aldrich (St. Louis, MO, USA). Other chemicals were procured from Bendosen Chemicals Malaysia (Kuala Lumpur, Malaysia) and were used as received.

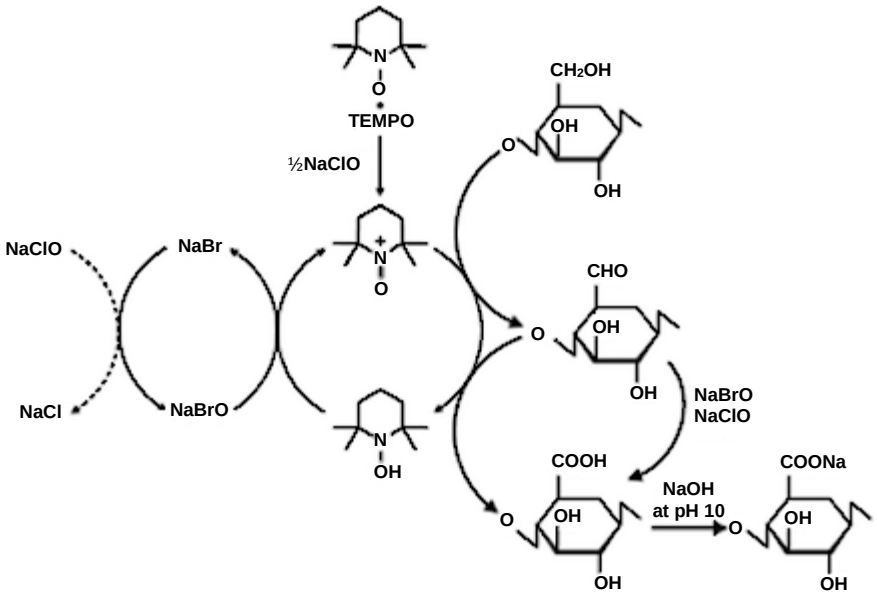

Fig. 1. Regioselective oxidation of cellulose by TEMPO-mediated oxidation (Johnson *et al*. 2009)

Isolation of Nanocrystalline Cellulose (NCC)

The OPEFB-NCC suspension was prepared by the sono-assisted TEMPO-mediated oxidation of unbleached OPFEB-Pulp, followed by ultrasonication of the resulting oxidized product (Rohaizu and Wanrosli 2017). OPEFB unbleached cellulose pulp was prepared using an environmentally benign process (Wan Daud *et al*. 2003) involving a sequence of water pre-hydrolysis of the OPEFB fibrous strands and soda pulping.

In brief, the isolation of OPEFB-NCC involved suspending OPEFB-pulp (3 g) in water (500 mL) containing 4-acetamido-TEMPO (0.115 g) and sodium bromide (0.37 g). A sodium hypochlorite solution (30 mL) was then added dropwise to the cellulose slurry followed by 0.5 M NaOH under continuous stirring so as to maintain a stable pH of 10.0 ± 0.1.The reaction was carried out in a glass reactor placed in a water ultrasonic bath (Branson 8510, Danbury, USA) with a frequency of 40 kHz at a constant temperature of 30 °C. After completion of the reaction (2 h), the pH of the solution was adjusted to 7 with 0.5 M HCl and separated by centrifugation (Kubota 5100, Tokyo, Japan) at 3500 rpm. The precipitate was dispersed in distilled water and centrifuged three more times to remove superfluous acids, inorganic salts, and TEMPO, resulting in a water-insoluble fraction of oxidized OPEFB-pulp. This material was re-dispersed by an ultrasonic probe (Branson Sonifier 450) at 20 kHz for 30 min. The OPEFB-NCC supernatant was obtained by centrifuging the colloidal suspension at 3500 rpm for 1 h followed by filtration through a 15 µm filter to remove microcontaminants and fibrous aggregates.

Fabrication of PLA-NCC Bionanocomposite Film

Prior to the fabrication of the PLA-NCC bionanocomposite film, water was first removed from the OPEFB-NCC by a "modified" oven-drying technique that is described

in Indarti *et al.* (2015). In brief, the aqueous NCC emulsion is dried in an air circulated oven at 50 °C until the suspension becomes viscous, after which it is taken out and ground in a mortar and placed back in the oven, with the process repeated until complete drying as indicated by a constant moisture content. A uniform particle size of an average of 40 μm was obtained after a final grinding and sieving. Before mixing with the PLA, the OPEFB-NCC was sonicated in 10 mL chloroform at various concentrations (0.01 to 0.20 g/mL) using an ultrasonic probe (Branson Sonifier 450) in an ice-bath (to prevent overheating). TheNCC in chloroform suspension was then added to 20 mL PLA solution and stirred for 4 h, after which it was then cast on a flat glass with 0.03 to 0.05 mm casting thickness and left to dry at room temperature for 24 h. The dry films obtained were peeled off and stored in a desiccator at room temperature for further analysis and characterization. The obtained PLA-NCC bionanocomposites were denoted as PLA-NCC1, PLA-NCC3, PLA-NCC5, PLA-NCC10, and PLA-NCC20 according to the OPEFB-NCC loading levels.

Characterization of PLA-NCC Bionanocomposite Film

Electron microscopy (SEM and TEM)

Morphological analysis were carried out using TEM (Philips CM12 with Docu Version 3.2 image analyzer, Amsterdam, Holland) and SEM (EVO® MA10, Carl Zeiss NTS GmbH, Oberkochen, Germany) with the latter used to analyze the morphology of a cryo-fractured film. For the SEM analysis, samples were sputter-coated with gold before the microscopic observations were obtained at an accelerating voltage of 10 kV. In the TEM analysis, drops of the suspension (0.01% w/v) were deposited on carbon-coated electron microscope grids and allowed to dry. The sample was stained with phosphotungstic acid (approximately 2 wt%) for 30 s. Sample dimensions were measured directly from the TEM and SEM micrographs, and the results were based on a mean of 100 measurements.

Fourier transform infrared (FTIR) spectroscopy analysis

FTIR spectra were recorded with a Nicolet iS10 (Thermo Scientific, Madison, USA) FTIR spectrophotometer in ATR (Attenuated Total Reflectance) modality within the range of 600 to 4000 cm^{-1} and a 4 cm^{-1} resolution.

Differential scanning calorimetry (DSC)

The crystallization and melting behaviour of the PLA-NCC bionanocomposite were observed with a DSCinstrument (DSC-6, Perkin Elmer, Waltham, USA) under a nitrogen atmosphere at a heating rate of 10°C/min. A sample mass of approximately 8 mgwas placedin a sealedDSCcrimp pan and scanned in the range of 30 to200°C. The degree of crystallization in the bionanocomposites was calculated by the following equation,

$$X_c(\%) = \frac{\Delta H_m}{\omega \Delta H_{mo}} \text{ x } 100\% \quad (1)$$

where ω is the weight fraction of the PLA in the biocomposite and ΔH_{mo} is the melting enthalphy of the purely crystalline PLA sample, ~93.0 J/g (Martin and Avérous 2001).

Mechanical properties measurement

The tensile strength, elongation at break, and Young's modulus of all the films were measured using a Texture Analyzer TA-XT Plus (Hamilton, USA) according to EN ISO 527-1 (1996). The tests were performed on rectangular sample ($100 \times 10 mm^2$) with a fixed crosshead rate of 10 mm/min, a load cell of 50 N, and initial gauge of 60 mm. The thickness of the samples was determined before the tests and varied between 40 to 60 µm. The measurements were conducted at room temperature, and the results were taken as an average of five replicates.

RESULTS AND DISCUSSION

Morphological Analysis of PLA-OPEFB NCC Bionanocomposite

Prior to fabrication of PLA-NCC bionanocomposite film, the dried OPEFB-NCC was redispersed in chloroform. The duration between redispersion and casting was very crucial; if the suspension was not utilized within 15 min, the particles started to sediment. To ensure maximum dispersion, the OPEFB-NCC suspension was immediately used after redispersion.However, TEM observations showed that even this technique did not completely disperse the OPEFB-NCC into individual crystals (Fig. 2a). These results are supported by Fortunati *et al*. (2012b), who studied the preparation of the PLA/cellulose composites using cellulose nanocrystal (CNC) isolated from MCC by sulphuric acid hydrolysis. At a molecular level, duringdrying, the OPEFB-NCC lost the free and bound water, which caused the crystals to come into very close contact, resulting in the formation of hydrogen bonds and, consequently, particle agglomeration. According to Lindström *et al*. (2005), the redispersion (van der Waals) forces needed to completely separate the crystal aggregates must be strong enough to overcome the hydrogen bonds, otherwise agglomerates tend to occur.

The agglomeration of OPEFB-NCC crystals in the suspension form was, as expected, carried over into the PLA-OPEFB-NCC film, as observed *via* SEM (Fig. 2b). At 500X magnification, it was impossible to detect nanoparticles. Hence, the observed particles were agglomerates of OPEFB-NCC with an average diameter of 13.7 µm.

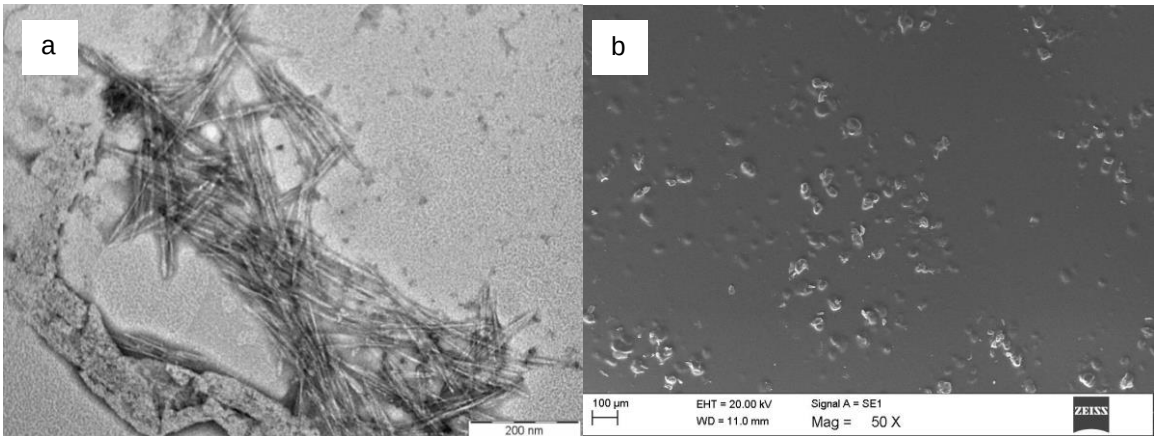

Fig. 2. (a) TEM of redispersed OPEFB-NCC in chloroform and (b) SEM of PLA-OPEFB NCC bionanocomposite with 5% OPEFB-NCC

Figure 3 shows the morphology of the cryo-fractured surface of PLA-NCC with various amounts of NCC. The SEM micrographs indicated the presence of small flakes (indicated by red arrows) on the surface of the bionanocomposite, with the numbers of flakes increasing at higher NCC content. These flakes comprised the agglomerated OPEFB-NCC particles that came from the redispersed OPEFB-NCC suspension; they had a very compact structure and lacked interfacial adhesion to the PLA matrix (Fortunati *et al*. 2012b). In addition, the presence of irregular outcroppings and holes on the surface of the PLA NCC matrix (white arrows) were also observed. These defects probably arose from the weak compatibility of NCC and PLA, causing voids and cracks around the flakes.

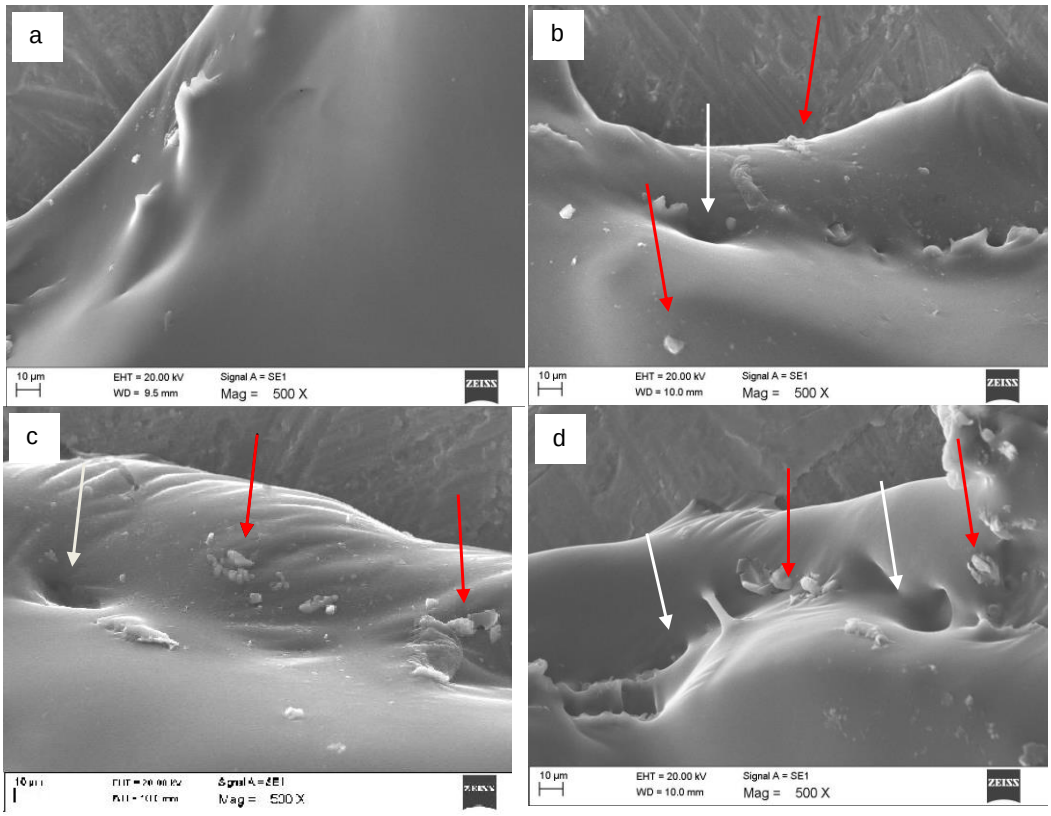

Fig. 3. SEM images of fracture surfaces for neat PLA (a), PLA-NCC 1 (b), PLA-NCC3 (c), and PLA-NCC5 (d) biocomposites at 500x magnification

These morphological analyses suggested that it was important to mantain NCC dispersion during biocomposite preparation by solvent casting. Even though NCC existed as aggregates, it did not seriously impact the properties of the biocomposite film because of its small size and good distribution.

FTIR Spectral Analysis of PLA-OPEFB Bionanocomposite

Figure 4 shows the FTIR spectra for the OPEFB-NCC, neat PLA, and PLA-NCC bionanocomposites. The spectrum of OPEFB-NCCwas similar to that of oil palm empty fruit bunch microcrystalline cellulose (OPEFB-MCC) as reported by Wanrosli *et al.* (2011). There were noteworthy vibration bands at 3700 to 3200 cm^{-1} and 2900 cm^{-1}, which are characteristic of the –OH stretching vibration and C–H stretching, respectively. An

exception was the presence of a strong 1730 cm^{-1} signal, corresponding to the carbonyl (C=O) stretching peak due to –COOH groups formed during TEMPO oxidation (Saito *et al*. 2006). The peak that appeared at 1749 cm^{-1}, resulting from the stretching of carbonyl C=O, was of particular importance for neat PLA (Qu *et al*. 2010).

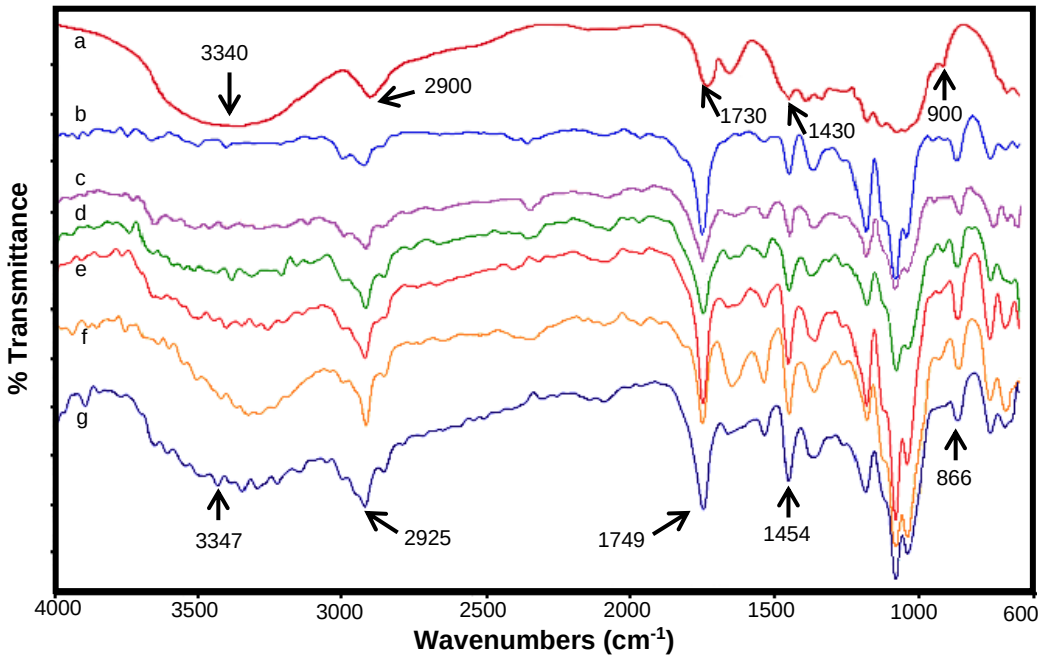

Fig. 4. FTIR spectra of (a) NCC, (b) neat PLA, and bionanocomposite films (c) PLA-NCC1, (d) PLA-NCC3, (e) PLA-NCC5, (f) PLA-NCC10, and (g) PLA-NCC20

After mixing with PLA, the OPEFB-NCC peaks no longer existed and were replaced by peaks belonging to the PLA component (Fig. 4). The amount of OPEFB-NCC was too low to have a substantial influence on the chemical composition of the bionanocomposite, *i.e*. it was masked by the PLA peaks. However, at higher amounts of OPEFB-NCC (Fig. 4f), there were changes in the shape of the peak at 2925 cm^{-1}. The broadening of the peak at 2925 cm^{-1} was probably due to the influence of the NCC particles, where at 2900 cm^{-1} there was also a peak belonging to the OPEFB-NCC, leading to overlapping peaks. In addition, both peaks at 1749 cm^{-1} and 3347 cm^{-1} became broader with increased OPEFB NCC loading.

Furthermore, because there were no new peaks in all of the PLA-OPEFB NCC bionanocomposites, it can therefore be assumed that the incorporation of the OPEFB-NCC was based on a physical rather than chemical interaction.

Table 1. Thermal Properties and Crystallinity of the PLA-NCC Biocomposites

Sample	$T_{g,mid}$ (°C)	T_c (°C)	T_m (°C)	ΔH_m (J/g)	X_c (%)
Neat PLA	65.35	106.70	167.32	33.12	35.61
PLA-NCC1	64.35	103.03	167.66	33.98	36.91
PLA-NCC3	64.39	103.04	167.98	33.76	37.42
PLA-NCC5	65.69	106.04	168.66	33.87	38.34
PLA-NCC10	67.44	98.42	167.52	37.33	44.60
PLA-NCC20	68.12	94.16	166.89	33.49	45.02

T_g, glass temperature; T_c, crystallization temperature; T_m, melt temperature; ΔH_m, melt enthalpy from the heating step; X_c, degree of crystallization

Thermal Properties of PLA OPEFN-NCC Bionanocomposites

The thermal properties as evaluated by DSC of unannealed neat PLA (first heating run) and its bionanocomposite film showing the three thermal phenomena of glass transition (T_g), crystallization temperature (T_c), and melting temperature (T_m) are illustrated in Table 1. These results are typical of a semi-crystalline polymer such as PLA (Suryanegara *et al.* 2010).

The T_g of the bionanocomposites did not change considerably with respect to the polymer matrix except at higher OPEFB-NCC additions. This effect was believed to result from the increase in the crystallinity of the bionanocomposite, which inhibited the mobility of the PLA molecular chains.With increasing OPEFB-NCC content, the crystallization temperature (T_c) shifted to lower temperatures, and crystallinity (X_c) increased. These observations can be explained by the two controlling factors that govern the crystallization process of any polymeric system, as suggested by Cheng *et al*. (2009). First, the additive/filler has a nucleation effect that enhances crystallization, resulting in an increase in T_c. Secondly, the additive/filler hinders the migration and diffusion of the polymeric molecular chains to the surface of the growing face of the polymer crystal in the composite, which inhibits the crystallization and lowers the T_c.

In the context of the present study, the presence of OPEFB-NCC yielded both positive and negative effects. It acted as a nucleating agent for the crystallization, but it also hindered the migration and diffusion of the PLA molecular chains in the bionanocomposite, leading to a decrease in T_c. The addition of 10% OPEFB NCC was the limiting factor, after which the effect was much less noticeable. For example, the T_c was only reduced to 4 °C above 10% OPEFB NCC. The T_c was 9 °C with 0% to 10% OPEFB NCC, while X_c increased by 0.4% and 9%, respectively.

The melting temperature (T_m) was observed as an endothermic peak in the vicinity of 167 °C for all PLA-OPEFB bionanocomposites. There was a strong relationship between T_m and size and perfection of the crystallites (Frone *et al*. 2013), and the T_m obtained in this study was more or less constant. These results suggest that the crystalline structure of all bionanocomposites was almost the same.

Table 2. Mechanical Properties of theNeat PLA and PLA/NCC Nanocomposite Films

Sample	Tensile Strength (MPa)	Elongation at Break (%)	Young's Modulus (GPa)
Neat PLA	44.31 ± 1.48	1.74 ± 0.04	2.55 ± 0.03
PLA-NCC1	32.83 ± 2.33	1.67 ± 0.21	1.99 ± 0.11
PLA-NCC3	33.42 ± 3.00	1.80 ± 0.02	1.86 ± 0.19
PLA-NCC5	26.22 ± 2.19	1.46 ± 0.01	0.87 ± 0.11
PLA-NCC10	19.46 ± 1.73	0.88 ± 0.05	1.02 ± 0.08
PLA-NCC20	14.04 ± 1.65	0.69 ± 0.18	0.98 ± 0.41

Mechanical Properties

The mechanical properties of neat PLA and PLA bionanocomposites were evaluated in terms of tensile test, elongation at break, and Young's modulus. Their mean and standard deviations are summarized in Table 2. All properties initially decreased with NCC addition, followed by a leveling-off until 3% loading, after which they decreased with further increases in NCC. Haafiz *et al.* (2013) reported similar results when using MCC as a reinforcement in PLA. The performance of reinforced materials relies on the efficiency with which mechanical stress is transferred from an external energy source to the reinforcing phase in the matrix, which in turn is a function of the amount and quality of the interfacial area between the reinforcing agent and the matrix (Klemm *et al*. 2011). This effect is related to several factors such as particle agglomeration, lack of dispersion, and weak interaction between the agent and matrix (Fortunati *et al*. 2012b), all of which probably contributed to the observed mechanical properties of the OPEFB-NCC PLA bionanocomposites in this study.

The occurrence of OPEFB-NCC agglomeration in the PLA matrix was shown in Fig. 2b. Because of this agglomeration, only a limited network structure was formed that could provide the reinforcing effects of the NCC, thus reducing both the modulus and strength of the bionanocomposite film. The cryo-fractured morphology of the PLA OPEFB-NCC samples (Fig. 3) indicated the presence of small flakes on the surface of the bionanocomposite; these flakes were evidence of the lack of interfacial affinity between the OPEFB-NCC and the PLA matrix. Irregular outcroppings and holes on the surface of PLA OPEFB-NCC matrix (Fig. 3) also resulted from the agglomeration, and these defects demonstrated the poor interfacial adhesion between the OPEFB-NCC and the PLA matrix. As a result, there was inefficient stress transfer to the OPEFB-NCC, which acted as the load bearing entity, leading to low strength values (Mathew *et al*. 2005). It can be argued that OPEFB-NCC with a relatively high aspect ratio of 45 could absorb the mechanical stress, thus providing more efficient strengthening. However, particle agglomeration, poor dispersion, and inadequate compatibility has probably overridden these positive aspects, leading to adverse effects on the mechanical properties.

CONCLUSIONS

1. Nanocrystalline cellulose (OPEFB-NCC) was extracted from oil palm empty fruit bunch *via* the tempo-oxidation process following utrasonication.

2. Bionanocomposites of PLA with unmodified OPEFB-NCC filler loading levels of up to 20% were fabricated using the solvent casting method.
3. The absence of new FTIR peaks in all of the PLA-OPEFB NCC bionanocomposites suggested that the incorporation of the OPEFB-NCC was based on a physical but not chemical interaction.
4. DSC analysis showed that the melting temperature T_g of PLA-OPEFB NCC film did not change markedly except at higher OPEFB-NCC additions, while the crystallization temperature (T_c) was shifted to lower temperatures. Crystallinity (X_c) increased with increasing OPEFB-NCC content.
5. The presence of small flakes on the surface of the bionanocomposite suggested a rather weak compatibility between the OPEFB-NCC and PLA. These observations help to account for the decrease in the modulus and tensile strength of the bionanocomposite.

ACKNOWLEDGMENTS

The authors express their gratitude to Universiti Sains Malaysia for the Research UniversityGrant No. 1001/PTEKIND/814240 and the Ministry of Research, Technology and Higher Education of Indonesia for sponsoring the postgraduate study of Eti Indarti.

REFERENCES CITED

Avérous, L., and Halley, P. J. (2009). "Biocomposites based on plasticized starch," *Biofuels, Bioproducts and Biorefining* 3, 329-343. DOI: 10.1002/bbb.135

Beck-Candanedo, S., Roman, M., and Gray, D. G. (2005). "Effect of reaction conditions on the properties and behavior of wood cellulose nanocrystal suspensions," *Biomacromolecules* 6, 1048-1054. DOI: 10.1021/bm049300p

Bondeson, D., Mathew, A., and Oksman, K. (2006). "Optimization of the isolation of nanocrystals from microcrystalline cellulose by acid hydrolysis," *Cellulose* 13, 171-180. DOI: 10.1007/s10570-006-9061-4

Cheng, Q., de Vallance, D., Wang, J., and Wang, S. (2011). "Advanced cellulosic nanocomposite material,"in: *Advances in Composite Materials for Medicine and Nanotechnology*, Brahim Affat (ed.), InTech, Rijeka, Croatia, pp. 547-564. DOI: 10.5772/14050

Cheng, Q., Wang, S., and Rials, T. G. (2009). "Poly (vinyl alcohol) nanocomposites reinforced with cellulose fibrils isolated by high intensity ultrasonication," *Composites Part A: Applied Science and Manufacturing* 40(2), 218-224. DOI: 10.1016/j.compositesa.2008.11.009

EN ISO 527-1. (1996). "Plastics—Determination of tensile properties – Part 1: General principles," International Organization for Standardization, Geneva, Switzerland.

Fortunati, E., Armentano, I., Zhou, Q., Iannoni, A., Saino, E., Visai, L., Berglund, L. A., and Kenny, J. M. (2012b). "Multifunctional bionanocomposite films of poly(lactic acid), cellulose nanocrystals and silver nanoparticles," *Carbohydrate Polymers* 87(2), 1596-1605. DOI: 10.1016/j.carbpol.2011.09.066

Fortunati, E., Peltzer, M., Armentano, I., Torre, L., Jiménez, A., and Kenny, J. M. (2012a). "Effects of modified cellulose nanocrystals on the barrier and migration properties of PLA nano-biocomposites," *Carbohydrate Polymers* 90(2), 948-956. DOI: 10.1016/j.carbpol.2012.06.025

Frone, A. N., S. Berlioz, S., Chailan, J. F., and Panaitescu, D. M. (2013). "Morphology and thermal properties of PLA-cellulose nanofibers composites," *Carbohydrate Polymers* 91(1), 377-384. DOI: 10.1016/j.carbpol.2012.08.054

Goussé, C., Chanzy, H., Excoffier, G., Soubeyrand, L., and Fleury, E. (2002). "Stable suspensions of partially silylated cellulose whiskers dispersed in organic solvents," *Polymer* 43(9), 2645-2651. DOI: 10.1016/S0032-3861(02)00051-4

Haafiz, M. K. M., Hassan, A., Zakaria, Z., Inuwa, I. M., Islam, M. S., and Jawaid, M. (2013). "Properties of polylactic acid composites reinforced with oil palm biomass microcrystalline cellulose," *Carbohydrate Polymers* 98(1),139-145. DOI: 10.1016/j.carbpol.2013.05.069

Habibi, Y., Lucia, L. A., and Rojas, O. J. (2010). "Cellulose nanocrystals: Chemistry, self-assembly, and applications," *Chemical Reviews* 110(6), 3479-3500. DOI: 10.1021/cr900339w

Heux, L., Chauve, G., and Bonini, C. (2000). "Nonflocculating and chiral-nematic self-ordering of cellulose microcrystals suspensions in nonpolar solvents," *Langmuir* 16(21), 8210-8212. DOI: 10.1021/la9913957

Indarti, E., Marwan, and Wanrosli, W. D. (2015). "Thermal stability of oil palm empty fruit bunch (OPEFB) nanocrystalline cellulose: Effects of post-treatment of oven drying and solvent exchange techniques," *Journal of Physics: Conference Series* 622. DOI: 10.1088/1742-6596/622/1/012025

Johnson, R. K., Zink-Sharp, A., Renneckar, S. H., and Glasser, W. G. (2009). "A new bio-based nanocomposite: fibrillated TEMPO-oxidized celluloses in hydroxypropylcellulose matrix," *Cellulose* 16(2), 227-238. DOI: 10.1007/s10570-008-9269-6

Klemm, D., Kramer, F., Moritz, S., Lindstrom, T., Ankerfors, M., Gray, D., Dorris, A. (2011). "Nanocelluloses: A new family of nature-based materials," *Angewandte Chemie International Edition* 50(24), 5438-5466. DOI: 10.1002/anie.201001273

Lin, N., Chen, G. J., Huang, J., Dufresne, A., and Chang, P. R. (2009). "Effects of polymer-grafted natural nanocrystal on structure and mechanical properties of poly(lactic acid): A case of cellulose whisker-*graft*-polycaprolactone," *Journal of Applied Polymer Science* 113(5), 3417-3425. DOI: 10.1002/app.30308

Lindström, T., Wågberg, L., and Larsson, T. (2005). "On the nature of joint strength in paper – A review of dry and wet strength resins used in paper manufacturing," in: *Proc. 13th Fundamental Research Symposium*,Cambridge, UK, pp. 457-562.

Mandal, A., and Chakrabarty, D. (2011). "Isolation of nanocellulose from waste sugarcane bagasse (SCB) and its characterization,"*Carbohydr. Polym.* 86, 1291-1299.

Martin, O., and Avérous, L. (2001). "Poly(lactic acid): Plasticization and properties of biodegradable multiphase systems," *Polymer* 42(14), 6209-6219. DOI: 10.1016/S0032-3861(01)00086-6

Mathew, A. P., Oksman, K., and Sain, M. (2005). "Mechanical properties of biodegradable composites from poly lactic acid (PLA) and microcrystalline cellulose (MCC),"*Journal of Applied Polymer Science* 97(5),2014-2025. DOI: 10.1002/app.21779

Miao, C., and Hamad, W. Y. (2013). "Cellulose reinforced polymer composites and nanocomposites: a critical review," *Cellulose* 20(5), 2221-2262. DOI: 10.1007/s10570-013-0007-3

Qu, P., Gao, Y., Wu, G. F., and Zhang, L. P (2010). "Nanocomposite of poly(lactic acid) reinforced with cellulose nanofibrils," *BioResources* 5(3), 1811-1823. DOI: 10.15376/biores.5.3.1811-1823

Raquez, J. M., Habibi, Y., Murariu, M., and Dubois, P. (2013). "Polylactide (PLA)-based nanocomposites," *Progress in Polymer Science* 38(10-11), 1504-1542. DOI: 10.1016/j.progpolymsci.2013.05.014

Rohaizu, R. and Wanrosli, W. D. (2017). "Sono-assisted TEMPO oxidation of oil palm lignocellulosic biomass for isolation of nanocrystalline cellulose," *Ultrasonics Sonochemistry* 34, 631-639. DOI: 10.1016/ j.ultsonch.2016.06.040

Saito, T., Nishiyama, Y., Putaux, J. L., Vignon, M., and Isogai, A. (2006). "Homogeneous suspensions of individualized microfibrils from TEMPO-catalyzed oxidation of native cellulose," *Biomacromolecules* 7(6), 1687-1691. DOI: 10.1021/bm060154s

Shirai, M. A., Grossmann, M. V. E., Mali, S., Yamashita, F., García, P. S., and Müller, C. M. O. (2013). "Development of biodegradable flexible films of starch and poly(lactic acid) plasticized with adipate or citrate esters," *Carbohydrate Polymers* 92(1), 19-22. DOI: 10.1016/j.carbpol.2012.09.038

Suryanegara, L., Nakagaito, A. N., and Yano, H. (2010). "Thermo-mechanical properties of microfibrillated cellulose-reinforced partially crystallized PLA composites," *Cellulose* 17(4), 771-778. DOI: 10.1007/s10570-010-9419-5

Wan Daud, W. R., Leh, C. P., Zainuddin, Z., and Tanaka, R. (2003). "Optimization of soda pulping variable for preparation of dissolving pulps from oil palm fiber," *Holzforschung* 57, 106-113.

Wanrosli, W. D., Rohaizu, R., and Ghazali, A. (2011). "Synthesis and characterization of cellulose phosphate from oil palm empty fruit bunches microcrystalline cellulose," *Carbohydrate Polymers* 84(1), 262-267. DOI: 10.1016/j.carbpol.2010.11.032

Article submitted: March 25, 2016; Peer review completed: June 26, 2016; Revised version received and accepted: August 10, 2016; Published: August 25, 2016.
DOI: 10.15376/biores.11.4.8615-8626